Bull. Mater. Sci., Vol. 40, No. 7, December 2017, pp. 1481–1488
https://doi.org/10.1007/s12034-017-1504-z

Microstructure and mechanical properties of laminated Al–Cu–Mg composite fabricated by accumulative roll bonding

PARISA DARVISH MOTEVALLI and BEITALLAH EGHBALI*
Department of Materials Engineering, Sahand University of Technology, P.O. Box 51335-1996, Tabriz, Iran
*Author for correspondence (eghbali@sut.ac.ir)

MS received 21 April 2016; accepted 12 April 2017; published online 29 November 2017

Abstract. In the present research, laminated Al–Cu–Mg composite was processed by the accumulative roll bonding (ARB) method. Initially, aluminium, copper and magnesium strips were alternatively stacked together. Then these stacked strips were rolled at 150°C up to five ARB cycles. The microstructure of composites was studied by optical microscopy. Micro-hardness and tensile tests were conducted to evaluate mechanical properties of the processed composites. After the first cycle of ARB, it was observed that copper and magnesium layers were necked and fractured. With increasing ARB up to four cycles, laminated Al–Mg–Cu composite with homogeneous distribution of fragmented reinforcement in matrix was produced. It was observed that with increasing ARB up to four cycles the strength and micro-hardness of fabricated composites increased and elongation decreased at the same time. These differences in mechanical behaviour have been attributed to the microstructural aspects of the individual layers and the fragmentation processes.

Keywords. Laminated Al–Cu–Mg composite; microstructure; mechanical properties; accumulative roll bonding.

1. Introduction

Metal matrix composites (MMCs), because of their potential in designing light weight structures, have played a great role in the materials used in industries such as automotive and aerospace applications [1,2]. Among them, aluminium matrix composites (AMCs) are usually used in the industrial applications [3]. The traditional methods for fabricating AMCs include powder metallurgy (PM), squeeze casting, pressure-less infiltration [4] and spray forming. Lu *et al* [5] and other researchers processed AMCs by accumulative roll bonding (ARB), which is one of the severe plastic deformation methods proposed by Saito *et al* [6]. During ARB, a large strain can be introduced into the metallic sheet without any geometrical changes [7]. As reported by researchers [8–14], several kinds of laminated composites have been produced using the ARB process.

Mg alloy has only two-third of the aluminium's density and excellent damping capacity. Aluminium often shows a higher strength and a better formability than Mg [15]. On the other hand, Cu has a good formability and a good corrosion resistance [16]. The Al–Mg–Cu composite has modified properties compared with its metal components. In addition, Al–Mg–Cu composite is very attractive for potential applications of structural metals. Accordingly, the aim of the present research is to fabricate multilayer Al–Mg–Cu composite through the ARB process. The microstructural evolutions and mechanical properties of produced composites were investigated at different ARB cycles.

2. Experimental

2.1 *Material*

Commercially pure aluminium, copper and magnesium (AZ31) sheets of 0.5 mm thickness were used as base materials and were annealed for 2 h at 350, 480 and 400°C, respectively. The pieces of the sheets 35 mm in width and 120 mm in length were cut for use as starting materials.

2.2 *ARB process*

In order to maintain surface treatments, copper sheets were pickled in 100 ml nitric acid and 1 ml hydrochloric acid solution. Then, the Al, Cu and AZ31 sheet surfaces were cleaned by acetone. Three aluminium foils, one copper and one magnesium foils (as 5L composite) and two aluminium foils, one copper and one magnesium foils (as 4L composite) were roughened by a steel brush and then stacked in an alternating sequence to form a 'sandwich' with a total thickness of 2.5 and 2 mm, respectively. Preheating was applied on sandwiches. The 5L and 4L composites were kept in a furnace at 150°C for 15 min. The thickness reduction of the first cycle was 50%, which was applied in a single pass. The total equivalent strain (ε_t) of the ARB processing can be estimated as follows [6]:

$$\varepsilon_t = \{(2/\sqrt{3})\ln(1-50\%)\}n = 0.8n, \quad (1)$$

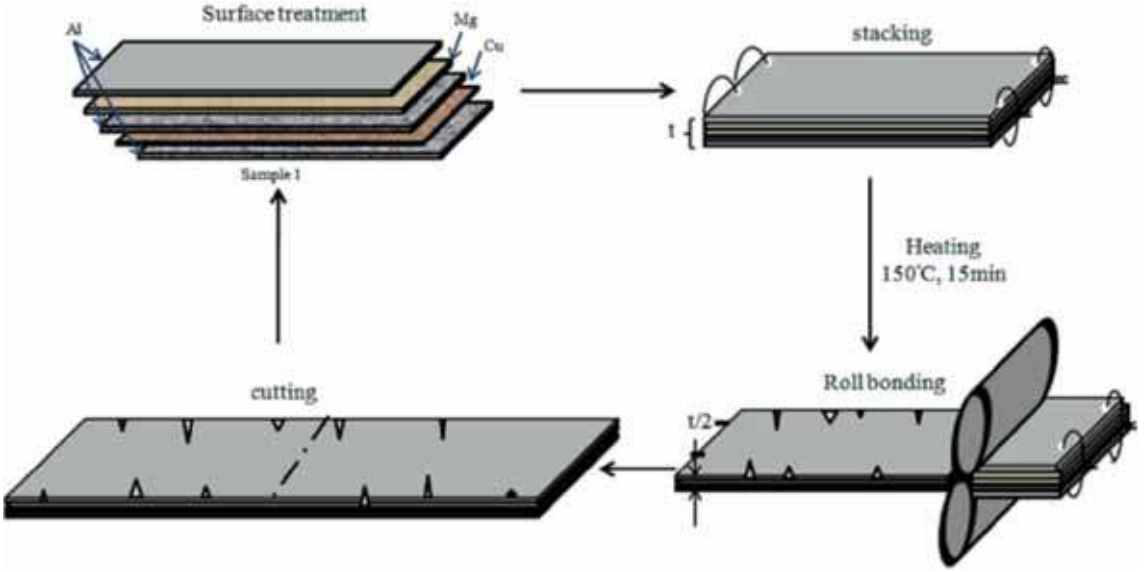

Figure 1. Schematic illustration showing the principle and procedure of the ARB process.

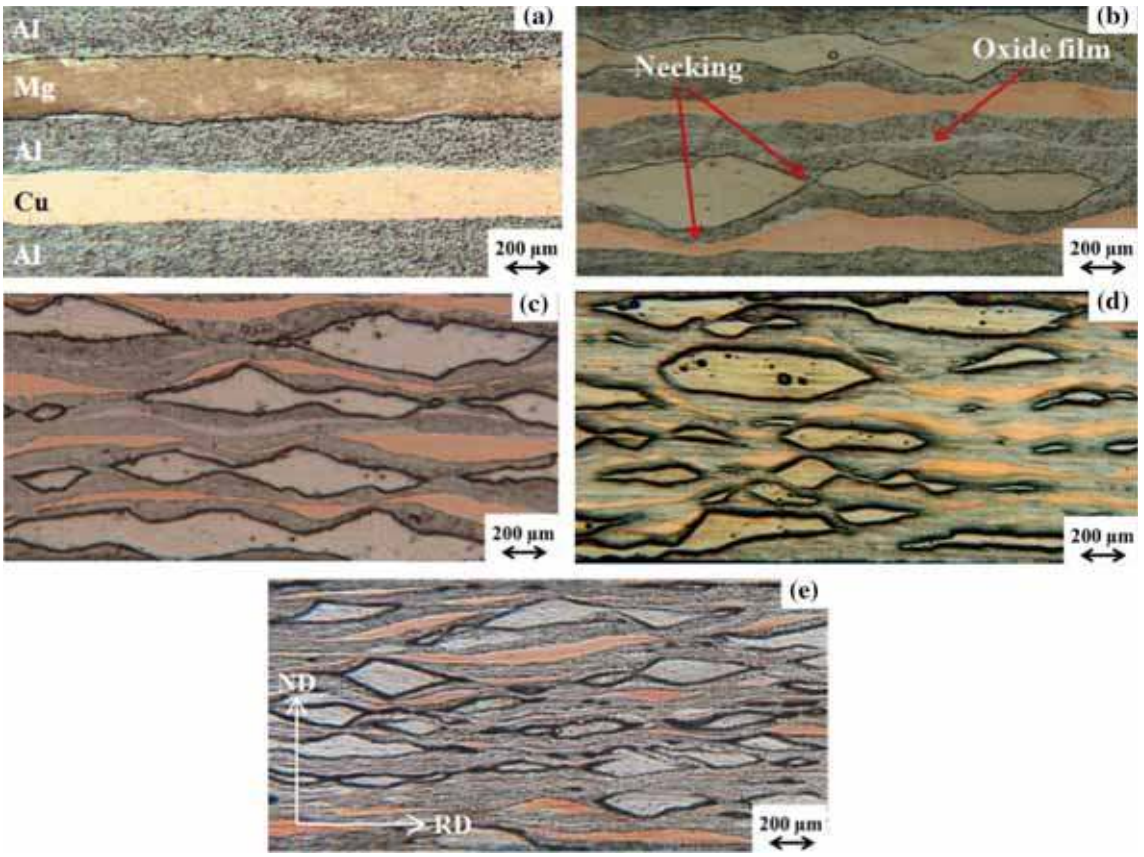

Figure 2. Optical image of ARB-processed sheets in (**a**) zeroth, (**b**) first, (**c**) second, (**d**) third and (**e**) fourth cycles, for 5L composite.

where ε_t is the total equivalent strain and n is the number of ARB passes. The samples were cut into half and the two halves were then placed together, thereby regaining their original thickness. Figure 1 shows the principle and procedure of the ARB processing. Excessively high total reduction, i.e., repetition times, can sometimes result in edge

cracks or centre fracture as shown in figure 1. This may be due to tensile stress caused by lateral spreading near the edges.

2.3 *Evaluation of microstructure and mechanical properties*

The microstructure of the Al–Cu–Mg composite in the rolling direction (RD) and normal direction (ND) was observed by optical microscope (OM) to investigate the effects of the number of ARB cycles on the Mg and Cu particles in the Al matrix. The composition profiles across the Al–Mg–Cu interface of the composite subjected to ARB were obtained by an energy-dispersive X-ray spectrometer (EDS) line scan analysis of a 4 μm line perpendicular to the Al–Mg–Cu interface. The phase evolution was identified using an EDS and an X-ray diffractometer (XRD). Diffraction patterns were recorded using a Philips X'Pert diffractometer employing Cu-K α at room temperature. The data were collected for diffraction angles $10° \leq \theta \leq 120°$, with a step width of 0.1° and a step time of 0.5 s. The diffraction was performed on the cross-sections of samples. Vickers microhardness (HV) test, using a load of 50 g for 10 s, was performed on the cross-section (RD–ND plane) through the thickness of the ARB-processed samples. The mean value of seven separated measurements was taken and reported at randomly selected points. The tensile test samples were machined from the ARB-processed strips, according to a half of ASTM-E8 standard, to get orientation along the RD. The gauge width and length of the tensile test samples were 6 and 25 mm, respectively. Tensile tests were conducted at the strain rate of 7×10^{-4} s^{-1} and room temperature. Tensile direction was parallel to the RD.

3. Results and discussion

3.1 *Microstructure evaluation*

Figures 2 and 3 show the optical micrographs of the cross-sectional interfaces of laminated Al–Mg–Cu composites processed for different ARB cycles. As seen, in the primary cycle all layers are in uniform shape. Because of low strain in the primary cycle (figures 2a and 3a), AZ31 and Cu layers were continuously deformed. These figures illustrate that the initial roll bonding process adopted in this research yields interfaces nearly free of pores, cracks or lateral delamination. Under ideal conditions, for two layers with the same mechanical properties, the interface is expected to be a straight line.

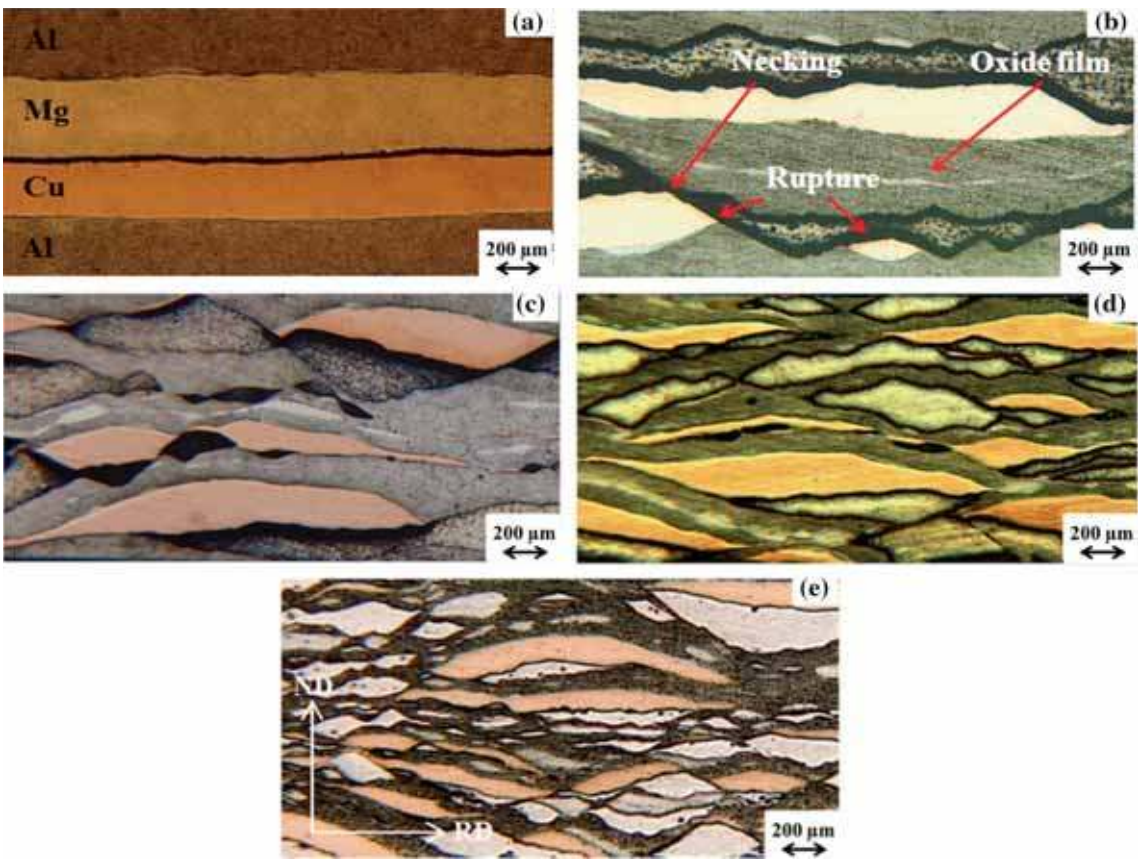

Figure 3. Optical image of ARB-processed sheets in (**a**) zeroth, (**b**) first, (**c**) second, (**d**) third and (**e**) fourth cycles, for 4L composite.

However, in the present composite, Al layer is softer than AZ31 and Cu layers. Therefore, further deformation made the hard layers (AZ31 and Cu) to neck and finally ruptured them. Accordingly, it can be seen that Al–Mg and Al–Cu interfaces are curved. These results are in agreement with those reported by Yu *et al* [17]. At the first ARB cycle, AZ31 and Cu were necked and fractured simultaneously in 5L (figure 2b). In 4L composite (figure 3b), Cu layer was ruptured (white area) and AZ31 layer was necked (dark area). During plastic co-deformation of different metals, different factors influence the plastic instability of layers besides difference in the mechanical properties of layers. With increasing number of ARB cycles, the Al–Al interfaces introduced by discontinuous oxide film were also clearly observed and showed that this layer was formed during pre-heating. It can be seen that as ARB proceeds, strain is increased and thickness of layers is decreased. After four cycles of ARB process, an AMC with a homogeneously distributed AZ31 and Cu fragments in the matrix was achieved (figures 2c–e and 3c–e).

Figure 4 shows the formation of shear bands after two ARB cycles. Some shear bands are distributed in the elongated Al, AZ31 and Cu layers. The localized deformation was restricted to the shear bands at an angle of about 42.4° to the RD. Previous works [12] showed that shear bands in the matrix around the interface of matrix and reinforcement move inside the hard phase due to its lower formability and thereby cause shear and separation in hard phases.

In the early stages of ARB process, the length of the AZ31 layers is more than the distance of shear bands, and consequently incoherent fragmentations along the layers are created; however, as ARB proceeds, AZ31 layers are traversed and shortened by shear bands. The microstructure of sheets, deformation conditions and difference in flow properties of neighbouring sheets influence the formation of shear bands [18]. Breakage regions create a void zone in matrix after formation of shear bands, which reduces strength and elongation [19]. These zones disappeared with matrix flowing.

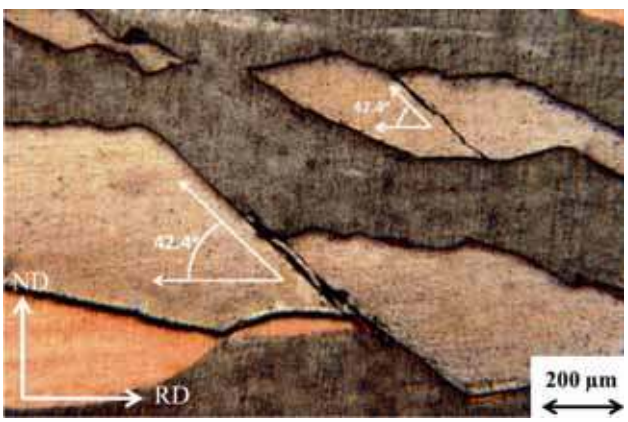

Figure 4. Optical micrograph of the shear bands at approximately 42.4° to rolling direction for second ARB cycle.

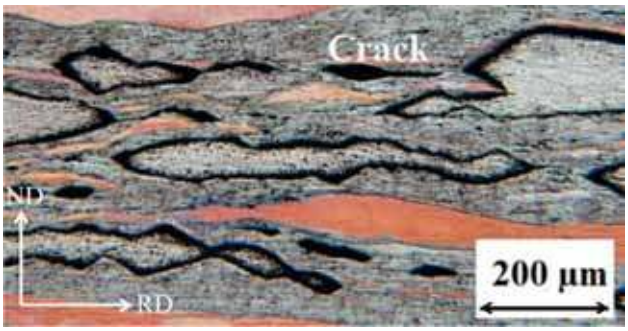

Figure 5. Optical microstructure of Al–Mg–Cu 5L composite after four ARB cycles.

Figure 5 shows a diagram of void zone forming and disappearing.

X-ray diffraction experiments were performed in order to identify the phases that are present in the composite. A total of three different phases were identified. Al, Mg and Cu were found to be the contributors in the diffraction pattern and no evidence of intermediate compound formation was found (figure 6). Intermetallic compounds were not formed due to the low temperature condition of experiments [20].

In the present research, the Al–Mg–Cu interface introduced by the sandwich preparation was placed at the inner part of the sheet and continuously strengthened by the ARB process. The intermix of Al, Mg and Cu atoms or the metallic bonding could be strongly intensified due to the repeated ARB process, which would further increases penetration of the atomic compounds. Moreover, lattice defects and the temperature increase caused by the ARB process can promote the inter-diffusion at the interface between dissimilar layers, which is similar to the mechanical alloying process [7].

Figures 7 and 8 show the SEM–EDS measurement across an inter-layer boundary for the Al–Mg and Al–Cu interfaces of 5L and Al–Mg, Al–Cu and Cu–Mg interfaces of 4L composites at the final ARB cycle. An 'X' shape of the EDS line scan illustrates that inter-diffusion of layer atoms and homogeneous bonding could be obtained.

3.2 *Mechanical properties*

3.2a *Tensile test*: Figure 9 shows the engineering stress–strain curves of five (5L) and four (4L) layered composites. It can be seen that the primary sandwich exhibits a significant increase in the yield stress and ultimate tensile strength while the elongations decrease; the first cycle has remarkable effect on the tensile strength, which is also proved by Pasebani and Toroghinejad [21].

It is seen that, before performing the second ARB cycle, both yield and tensile strength increase, for the composite in primary sandwich and the first cycle of ARB. Two different mechanisms have important roles in the strengthening of composite materials. These mechanisms are strain

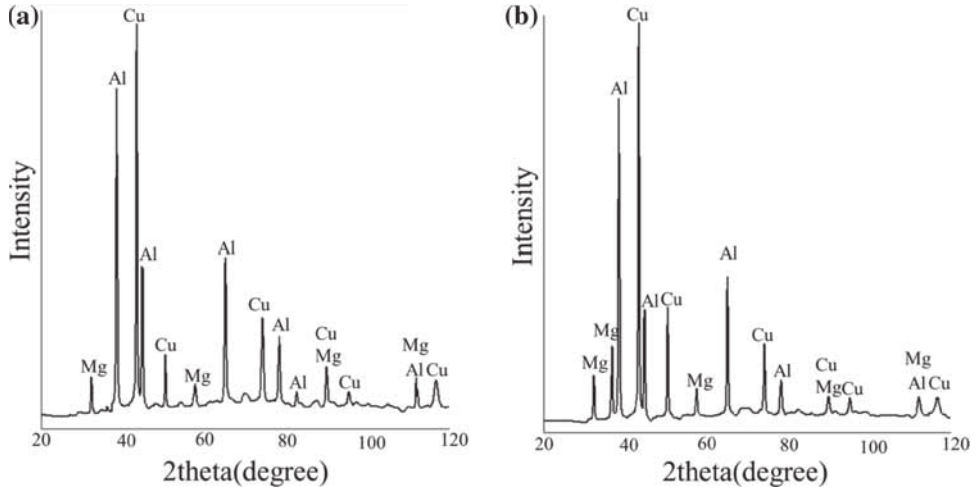

Figure 6. X-ray diffraction patterns for the Al–Mg–Cu composites: (**a**) 5L and (**b**) 4L.

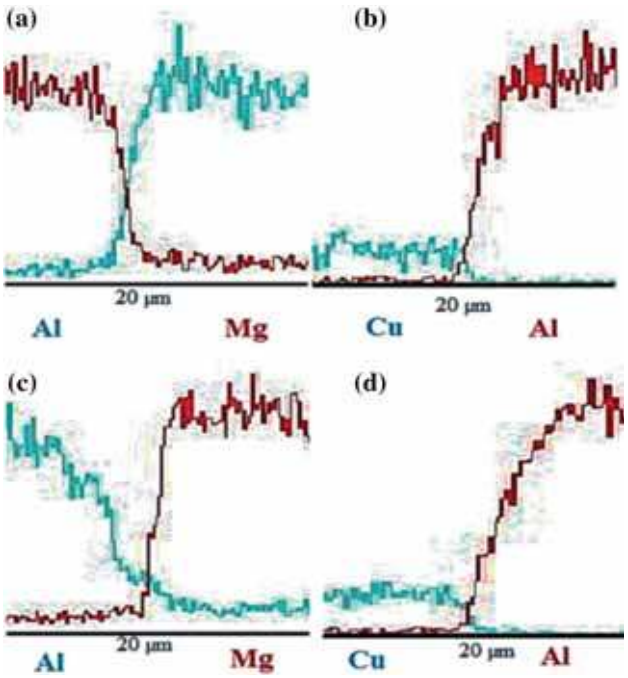

Figure 7. EDS line scan measurement in (a) Al–Mg, (b) Al–Cu primary sandwich and (c) Al–Mg, (d) Al–Cu fourth cycle ARB of 5L composite.

hardening or dislocation strengthening and grain boundary characteristics (high- and low-angle boundaries) [9,22]. In the initial cycles of ARB, the first mentioned mechanism plays a major role in raising the strength of composite material. Also, the second mechanism is predominant in the final stages of ARB processing [15].

According to observations of microstructure and tensile properties, the formation of cracks in shear region led to the decrease of mechanical properties. However, as ARB cycles increased, cracks were eliminated and tensile properties increased.

As reported by Shabani *et al* [3] the characteristic properties of reinforcement material such as size, shape, distribution and bonding quality between matrix and reinforcement can also alter the final strength of composite material. With increasing ARB cycles, reinforced material layers are changed from elongated to particle shape. This can increase the strength of the composite being deformed. Also, the distribution of reinforcement should be homogenous throughout the matrix in order to perceive isotropic property in the composite [23]. The change in the elongation values of composite can be attributed to some identified factors. With increasing the strain hardening rate and formation of shear bands during deformation, the elongation magnitude is diminished as a result of decreasing dislocation mobility [9]. The tensile properties of 5L composite are better than those of 4L composite, because deformation ability in Al is greater than in magnesium and copper metals; hence, interface bonding strengths of Al–Mg and Al–Cu are higher than that of Cu–Mg. In addition, as copper is stronger than Al and weaker than AZ31, bonding between AZ31 and Cu layers is weaker than bonding between AZ31 and Al layers, and Cu and Al layers.

3.2b *Microhardness*: Figure 10 illustrates the microhardness of Al, Mg and Cu layers at various ARB cycles. The initial increase of microhardness seems to be due to the strain hardening. In fact, initial reduction of grain size and increase of dislocation density inside the crystalline lattice lead to initial strain hardening and thereby a rapid increase in microhardness after initial ARB cycles [15]. Strain hardening rate was decreased at higher strains as a consequence of the dynamic balance between hardening and softening mechanisms [9]. It is obvious that staking fault energy of Cu is significantly lower than that of Al. Therefore, the dislocation cross-slip is extremely harder and consequently the work

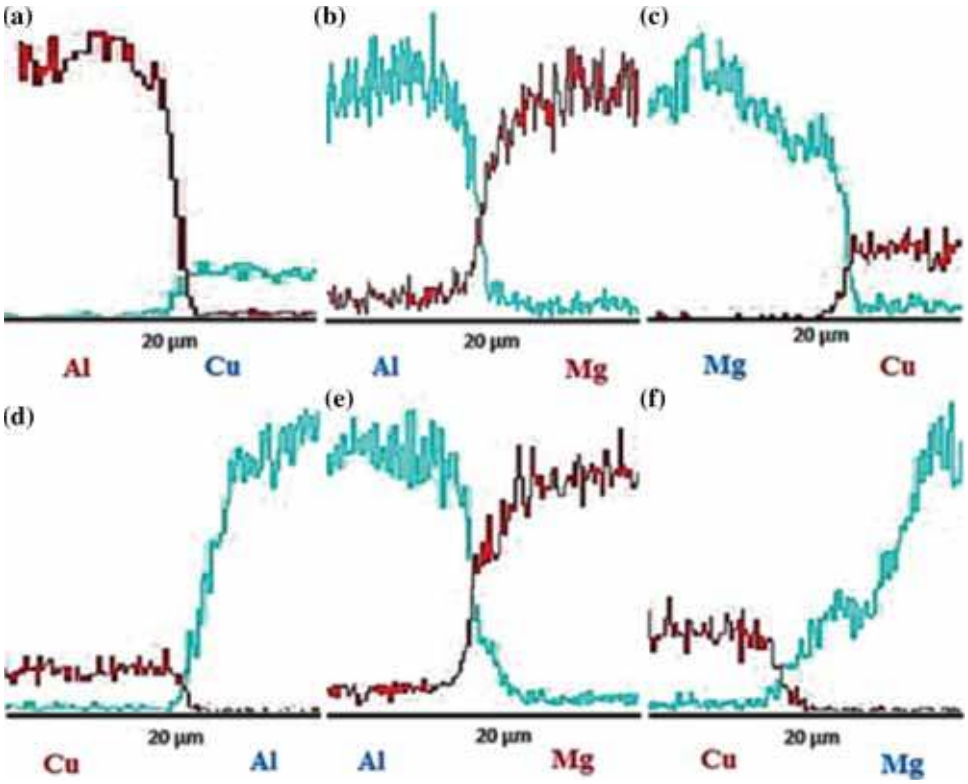

Figure 8. EDS line scan measurement in (a) Al–Cu, (b) Al–Mg, (c) Cu–Mg primary sandwich and (d) Al–Cu, (e) Al–Mg, (f) Cu–Mg fourth cycle ARB of 4L composite.

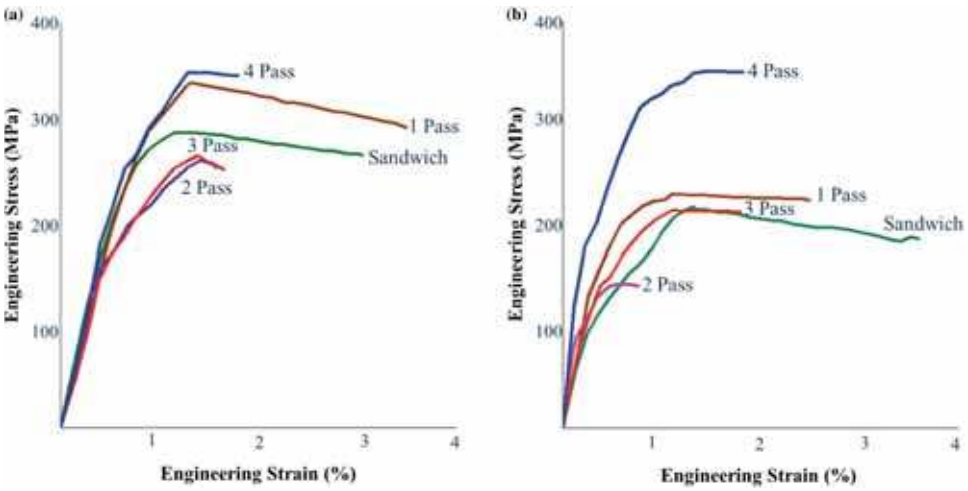

Figure 9. Engineering stress–strain diagrams: (**a**) 5L and (**b**) 4L composites.

hardening rate of Cu is higher than that of Al. In addition, stacking fault energy of AZ31 alloy is lower than that of Al and hence the microhardness of AZ31 layer is higher than that of Al layer [23].

3.2c *Fractography*: Figure 11 shows the fracture surfaces of Al–Mg–Cu composite. It is obvious that the presence of voids is related to the stress sate. Therefore, it can be inferred that if fracture is affected by shear stresses, voids are stretched and elliptic voids are formed in the fracture surface [24]. Voids were not observed in the magnesium and copper layers, thereby indicating that the fracture had cleavage characteristics. Finally, stretched voids in the shear stress direction were observed on the fracture surface of composite after four cycles. This can be considered as shear ductile fracture (figure 11b).

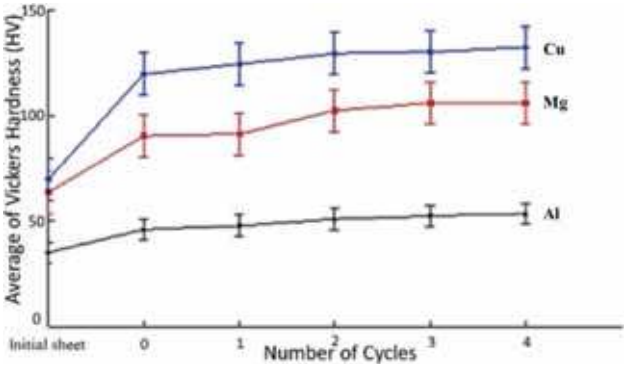

Figure 10. Variation of average microhardness with respect to accumulative strain in ARB.

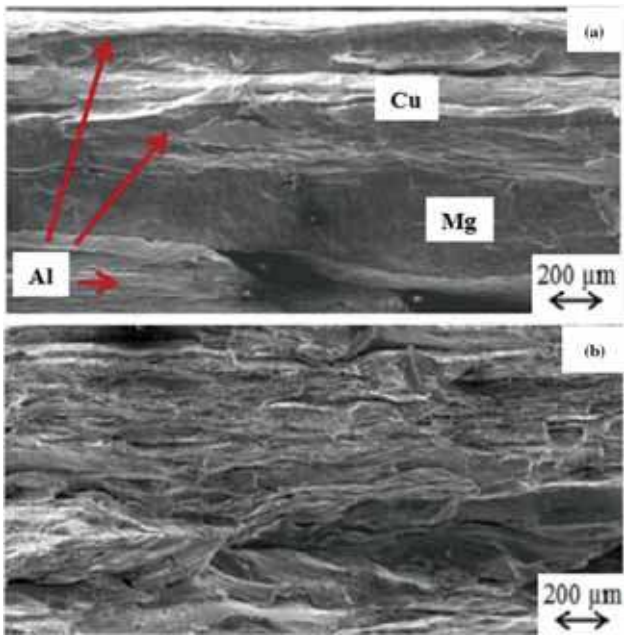

Figure 11. Fracture surface of Al/Mg/Cu 5L composite after the (**a**) zeroth and (**b**) fourth ARB cycle.

4. Conclusions

New AMCs with aluminium, magnesium and copper are fabricated through five cycles of ARB process. The microstructure evaluation and mechanical properties of the composites were investigated. The conclusions can be summarized as follows:

(1) The laminated Al–Mg–Cu composite was successfully processed by the ARB process. On increasing the number of ARB cycles, the distribution of the reinforcement layers in the aluminium matrix increased and after four ARB cycles a composite with homogeneously distributed reinforcing layers was produced.

(2) During ARB, in the aluminium–magnesium, aluminium–copper and magnesium–copper interfaces, no intermetallic compound was found but some intermixing occurred at the interfaces.

(3) With increasing ARB cycles, reinforced material layers changed from elongated to particle shape. This led to increase in strength of the composite being deformed.

(4) The microhardness of composites increases with increasing ARB cycles. Strain hardening and interaction of dislocations lead to plateau of microhardness curve in last cycles.

Acknowledgements

The authors would like to thank the research board of the Sahand University of Technology for the provision of research facilities used in this work.

References

[1] Li L, Nagai K and Yin F 2008 *Sci. Technol. Adv. Mater.* **9** 023001
[2] Scherm F, Völkl R, Van Smaalen S, Mondal S, Plamondon P, Espéranceb G L *et al* 2009 *J. Mater. Sci. Technol. A* **518** 118
[3] Shabani A, Toroghinejad M R and Shafyei A 2012 *J. Mater. Sci. Technol. A* **558** 386
[4] Huang X, Tsuji N, Hansen N and Minamino Y 2003 *Mater. Sci. Eng. A* **340** 265
[5] Lu C, Tieu K and Wexler D 2009 *J. Mater. Process. Technol.* **209** 4830
[6] Satio Y, Utsunomiya H, Tsuji N and Sakaki T 1999 *Acta Mater.* **47** 579
[7] Chang H, Zheng M Y, Xu C, Fan G D, Brokmeier H G and Wu K 2012 *Mater. Sci. Eng. A* **543** 249
[8] NasiriDehsorkhi R, Qods F and Tajally M 2011 *J. Mater. Sci. Technol. A* **530** 63
[9] Eizadjou M, Kazemi A, Talachi H, DaneshManesh, Shakur Shahabi H and Janghorban K 2008 *Compos. Sci. Technol.* **68** 2003
[10] Liu H S, Zhang B and Zhang G P 2011 *J. Mater. Sci. Technol.* **27** 15
[11] Zhang R and Acoff V L 2007 *Mater. Sci. Eng. A* **463** 67
[12] Min G, Lee J, Kang S and Kim H 2006 *Mater. Lett.* **60** 3255
[13] Danesh Manesh H and Karimi Taheri A 2003 *J. Alloys Compd.* **361** 138
[14] Yang D, Cizek P, Hodgson P and Wen C 2010 *Scr. Mater.* **62** 321
[15] Wu K, Chang H, Maawad E, Gan W M, Brokmeier H G and Zheng M Y 2010 *Mater. Sci. Eng. A* **527** 3073
[16] Alizadeh M and Talebian M 2012 *J. Mater. Sci. Eng. A* **558** 331
[17] Yu H, Tieu A K, Lu C, Liu X *et al* 2014 *Sci. Rep.* **4** Article no. 5017
[18] Toroghinejad M R, Ashrafizadeh F and Jamaati R 2013 *J. Mater. Sci. Eng. A* **561** 145

[19] Chen M C, Hsieh H C and Wu W 2006 *J. Alloys Compd.* **416** 169
[20] Mozaffari A, DaneshManesh H and Janghorban K 2010 *J. Alloys Compd.* **489** 103
[21] Pasebani S and Toroghinejad M R 2010 *Mater. Sci. Eng. A* **527** 491
[22] Mei-yan Z, Yuan-yuan L and Wei-ping C 2008 *Trans. Nonferrous Met. Soc.* **18** 309
[23] Viswanathan V, Laha T, Balani K, Agarwal A and Seal S 2006 *Mater. Sci. Eng. R* **54** 121
[24] Khorshid M T, Jahromi S A J and Moshksar M M 2010 *Mater. Des.* **31** 3880